Absorption effects in diffusing wave spectroscopy

Erick Sarmiento-Gomez,[1,3] Beatriz Morales-Cruzado,[2,4] and Rolando Castillo[1,*]

[1]Instituto de Física, Universidad Nacional Autónoma de México, P.O. Box 20-364, D. F. México 01000, Mexico

[2]Departamento de Óptica, INAOE, Luis Enrique Erro 1, Tonantzintla, Puebla, Mexico

[3]Present address: Instituto de Física "Manuel Sandoval Vallarta," Universidad Autónoma de San Luis Potosí, Alvaro Obregón 64, 78000 San Luis Potosí, S.L.P., Mexico

[4]Present address: Facultad de Ingeniería, Universidad Autónoma de San Luis Potosí, Alvaro Obregón 64, 78000 San Luis Potosí, S.L.P., Mexico

*Corresponding author: rolandoc@fisica.unam.mx

Received 25 March 2014; revised 4 June 2014; accepted 5 June 2014;
posted 9 June 2014 (Doc. ID 208862); published 16 July 2014

The effect of absorption in diffusing wave spectroscopy (DWS) was studied using an absorption-dependent diffusive equation for describing the light propagation within a turbid liquid where dielectric microspheres have been embedded. Here, we propose an expression for the time-averaged light intensity autocorrelation function that correctly describes the time fluctuations for the scattered light, in the regime where the diffusion approximation accurately describes the light propagation. This correction was suspected previously, but it was not formally derived from a light diffusive equation. As in the case of no absorption, we obtained that time fluctuations of the scattered light can be related to the mean square displacement of the embedded particles. However, if a correction for absorption is not taken into account, the colloidal dynamics can be misinterpreted. Experimental results show that this new formulation correctly describes the time fluctuations of scattered light. This new procedure extends the applicability of DWS, and it opens the possibility of doing microrheology with this optical method in systems where absorption cannot be avoided.

OCIS codes: (000.6590) Statistical mechanics; (290.1990) Diffusion; (290.4210) Multiple scattering; (290.7050) Turbid media.

http://dx.doi.org/10.1364/AO.53.004675

1. Introduction

Information about the static and dynamic properties of colloidal particles in liquid suspensions, artificially embedded or the product of self-assembly, is usually obtained from dynamic light scattering on length scales comparable to the size of these particles. In concentrated suspensions, this technique cannot be applied due to strong multiple scattering of light. In the early 1990s, diffusing wave spectroscopy (DWS) was introduced to deal with systems with strong multiple scattering, where a diffusion model can be used to describe the propagation of the light across the sample. Here, the sample is made of the fluid of interest, usually a complex fluid, and probe particles are incorporated into the fluid to scatter light. Using such a diffusion approximation, it is possible to connect the temporal field fluctuations of the scattered light emerging from the strong scattering media to the dynamic processes of the probe particles that scatter light moving within the complex fluid [1–5]. Although DWS does not yield explicit information on the q dependence of the so-called dynamic structure factor of the particles, it is capable of providing unique information on particle motion at very short time scales. Fluctuations of the scattered light measured in transmission result from the variation of the total path length by a wavelength of light. However, since light is scattered from a large number of particles, each individual particle must move only a small fraction of a wavelength for a cumulative

1559-128X/14/214675-08$15.00/0

change in the path length to be a full wavelength; DWS can probe motion on very short length scales, from ∼1 nm up to ∼1 μm [6]. At the end, the Brownian motion of probe particles incorporated in the fluid of interest, which does not scatter or absorb light, can be tracked with multiple dynamic light scattering; the particles in the fluid are in a concentration that makes it turbid. Photons are multiply scattered and lose their q-dependence, giving rise to instruments using only transmission or backscattering geometries. The temporal electric field fluctuations of the scattered light emerging from the turbid suspension, characterized by the time-averaged field autocorrelation function (ACF), $g_{(1)}(t) = \langle E(0)E^*(t)\rangle / \langle |E(0)|^2\rangle$, are connected to the motion of the particles in the fluid. The mean-squared displacement (MSD) of the probe particles can be determined by collecting the scattered intensity from a single speckle of scattered light over a sufficiently long collection period to allow the evaluation of the time-averaged light intensity ACF, $g_{(2)}(t)$. This measured ACF is related to $g_{(1)}(t)$ through the Siegert relation, $|g_{(2)}(t)| = 1 + \beta|g_{(1)}(t)|^2$, where β is an instrumental factor determined by the collection optics [2–4]. In a transmission geometry, the fluid under investigation with the incorporated particles can be treated as a slab with an infinite transverse extent and a thickness $L \gg l^*$, where l^* is the transport mean free path. After traveling distance $\approx l^*$ light is randomized, and the transport of light in a turbid medium can be described by the diffusion approximation [2–4]. In this case, the expression of the time-averaged field ACF, $g_{(1)}(t)$, is a function of the MSD, the wave vector of the incident light, k_0, and l^*, that is, $g_{(1)}(t) = g_{(1)}(\langle \Delta r^2(t)\rangle, k_0, l^*)$ [2–4]. Therefore, the MSD of the particles can be extracted from the experimental measurement of $g_{(1)}(t)$, if l^* is determined with an independent measurement. The MSD as a function of time brings information about the diffusion coefficient of the scattering particles in the fluid that is relevant for understanding the mechanisms that lead to anomalous diffusion and arrested motion common in structured, disordered, and fractal media. DWS has also been used as a noninvasive technique for monitoring biological activity [7–17]. On the other hand, from the MSD the complex rheological modulus $G^*(\omega)$ of the fluid can be obtained. This is an important application of the DWS for studying the microrheological properties of macroscopically homogeneous soft matter [6,18–25], such as suspension of colloids, proteins, virus, and wormlike micelle solutions, just to mention a few of them [6,18–25]. There have been several improvements of DWS to deal with complex fluids, such as the multispeckle DWS [26–28]. This method was developed for studying systems with a slowly evolving transient behavior, exhibiting both short and long relaxation times, up to the point that ergodicity of the media cannot be ensured. The use of a CCD camera as a multispeckle light detector allows the simultaneous calculation of several hundreds of correlation functions simultaneously. The multispeckle nature of the CCD camera detector means that a true ensemble average is calculated; no time averaging is necessary. However, present DWS development restrictions do not allow study of liquid systems that absorb or scatter light prior to incorporating the probe particles. Many potential biological systems, magnetic fluids, and suspensions embedded with metal nanoparticles have these features; thus, circumventing these restrictions might widen the use of DWS.

Absorption effects in DWS were first discussed by Weitz and collaborators [3,4], who pointed out that absorption exponentially attenuates light paths according to their path length, cutting off the longest paths; however, analytical results were not derived. Soon after, the hypothesis of an exponential attenuation of photon flux along the path length was confirmed by experiments [29–31] and by Monte Carlo simulations [32–34]. DWS experiments in conjunction with time-of-flight measurements have allowed estimation of optical absorption in a highly scattering media [35,36].

The main goal of this work is to study the effect of absorption in DWS describing the light propagation in a strong scattering media with the proper absorption-dependent diffusive equation. We propose an expression that correctly describes the time fluctuations for the scattered light. This correction was suspected previously, but it was not formally derived from a light diffusive equation. We present experimental results confirming that this formulation correctly describes the time fluctuations of the scattered light, and it is also able to properly extract the dynamics of the scattering particles. The present formulation extends the applicability of DWS to a new variety of systems where absorption cannot be neglected.

2. Theory

A. DWS without Absorption

In a DWS experiment coherent light is incident on one side of a planar sample of thickness $L \gg l^*$, and the scattered light is collected from a small area on the opposite side. A single photon passing through the sample undergoes numerous scattering events and loses its scattering angle dependence. This leads to instruments using only transmission or backscattering geometries. Photons emerge with a phase that depends of the total path length s. Under the assumption of independence of light paths, the normalized field ACF can be written as [2–4]

$$\begin{aligned} g_{(1)}(t) &= \frac{\langle E(0)E^*(t)\rangle}{\langle |E(0)|^2\rangle} \\ &= \int_0^\infty P(s)\, \exp\left[-\frac{k_0^2\langle \Delta r^2(t)\rangle s}{3l^*}\right] \mathrm{d}s \\ &= \int_0^\infty P(s)\, \exp\left[-\frac{2t}{\tau}\frac{s}{l^*}\right] \mathrm{d}s, \end{aligned} \tag{1}$$

where $E(t)$ is the scattered electric field, $P(s)$ is the path distribution function of scattered photons, k_0 is the wave number, and $\langle \Delta r^2(t) \rangle$ is the MSD of the scattering probe particles. In the last expression, we used $2t/\tau = k_0^2 \langle \Delta r^2 \rangle /3$. These equations can be related to the Brownian diffusion with $\langle \Delta r^2 \rangle = 6D_0 t$; $D_0 = k_B T/6\pi\eta a$ for spherical particles of radius a in a solvent with viscosity η at temperature T.

For length scales greater than l^*, light transport can be described by the diffusion equation:

$$\frac{\partial \mathcal{U}}{\partial t} = D_1 \nabla^2 \mathcal{U}, \tag{2}$$

where $\mathcal{U}$ is the energy density of light, that is, the number of photons per unit volume, and $D_1 = cl^*/3$ is the diffusion coefficient of light [37–40], and c is the speed of light in the medium. To calculate $P(s)$ in Eq. (1), Eq. (2) should be solved subject to the initial condition $\mathcal{U}(z,t) = \mathcal{U}_0 \delta(z - z_0, t)$ and to the boundary condition for $t > 0$,

$$\left(\mathcal{U} + \frac{2}{3} l^* \hat{n} \cdot \nabla \mathcal{U} \right) \Big|_{z=0,L} = 0. \tag{3}$$

z_0 is the distance into the sample from the incident surface to the place where the diffuse source is located, and $\hat{n}$ is the outward normal to the surface [4,41]. Since the net diffusing flux of light exiting the sample is zero, $g_{(1)}$ in transmission geometry can be finally written as

$$g_{(1)}(t) = \frac{\frac{L/l^*+4/3}{\alpha^*+2/3}\left[\sinh(\alpha^* x) + \frac{2}{3} x \cosh(\alpha^* x)\right]}{\left(1 + \frac{4}{9}x^2\right)\sinh\left(\frac{L}{l^*}x\right) + \frac{4}{3}x \cosh\left(\frac{L}{l^*}x\right)}, \tag{4}$$

where $x = [k_0^2 \langle \Delta r^2(t) \rangle]^{1/2}$ and $\alpha^* = z_0/l^*$.

B. DWS with Absorption

As pointed out before [3,4], absorption alters the distribution of light path lengths $P(s)$, attenuating the longer paths. Consequences of absorption can be easily determined by considering that absorption exponentially attenuates paths according to their path length. $P(s)$ is the path length distribution in the absence of absorption. The path length distribution in the presence of absorption will be $P(s)\exp(-s/l_a)$, where l_a is the absorption length of the sample; $\mu_a \equiv 1/l_a$, where μ_a is the absorption coefficient. Therefore, Eq. (1), for the case of a absorbing sample, takes the form

$$g_{(1)}(t) = \int_0^\infty P(s) \exp\left[-\left(\frac{2t}{\tau} + \frac{l^*}{l_a} \right) \frac{s}{l^*} \right] ds. \tag{5}$$

Time delay is shifted in the autocorrelation function by l^*/l_a. Although Eq. (5) has been employed before [35,36], a relation similar to Eq. (5) was not formally derived. This is of key importance for making microrheological measurements.

To include absorption effects in a DWS experiment, a diffusion equation with an absorption term has to be solved to get a correct path distribution function of scattered photons. Two different approaches can be found in the literature to obtain a diffusion equation for light propagation in a turbid media [37–40,42]. Both lead to the same equation, but with different definitions of the diffusion coefficient. In one the diffusion coefficient is independent of the absorption length, D_1, and in the other $D_2 = c(l^* + l_a)/3$. However, Monte Carlo simulations have revealed that the absorption-independent diffusion coefficient D_1 gives better agreement with theory than D_2 [38]. Accordingly, the diffusion equation including absorption effects must be written as

$$\frac{\partial \mathcal{U}}{\partial t} = D_1 \nabla^2 \mathcal{U} - \mu_a c \mathcal{U}. \tag{6}$$

This equation can be derived from the radiative transfer equation by considering a nearly isotropic light distribution and assuming that $l_a \gg l^*$ [41,43]. For calculating $P(s)$ in transmission geometry, we followed the same line of reasoning given in [3,4] but using Eq. (6). We will assume that all photons are initially scattered at a depth z_0 comparable with l^*, so that the initial condition for Eq. (6) is similar to the case of no absorption mentioned above, $\mathcal{U}(z,t) = \mathcal{U}_0 \delta(z - z_0, t)$. The boundary conditions are also given by Eq. (3) as in the no-absorption case, taking into account that there is no flux of diffusing photons entering or leaving the sample. As above, the field ACF can be calculated directly from the energy density of light in the Laplace domain with

$$g_{(1)}(t) = \left[\frac{\tilde{\mathcal{U}}(\mathbf{r}, p)}{\tilde{\mathcal{U}}(\mathbf{r}, 0)} \right]_{z=L}. \tag{7}$$

Here $\tilde{\mathcal{U}}$ is the Laplace transform of $\mathcal{U}$ and $p(t) = k_0^2 \langle \Delta r^2(t) \rangle /3l^*$. The solution of Eq. (6) is of the form $\mathcal{U} = v + \nu$, where

$$v = \frac{1}{2\sqrt{\pi D_1 t}} \exp\left[-\frac{(z - z_0)^2}{4D_1 t} \right] \exp[-\mu_a c t] \tag{8}$$

is the solution to the diffusion equation for an infinite medium that satisfies the mentioned initial condition [43–45]. In the Laplace domain, Eq. (8) takes the form

$$\tilde{v}(q) = \frac{\exp(-q|z - z_0|)}{2D_1 q}, \tag{9}$$

where $q^2 = (3/l^*)(p + \mu_a)$. The Laplace transform for the solution of the subsidiary equation for ν is

$$\tilde{\nu}(q) = A \sinh(qz) + B \cosh(qz), \tag{10}$$

where A and B are chosen so that the boundary conditions are satisfied at $z = 0$ and $z = L$. Finally, after long algebraic calculations, the expression for the

field ACF, in transmission geometry, can be obtained in the following form:

$$g_{(1)}(t) = \frac{\frac{(1+\frac{4}{9}\eta^2)\sinh(\frac{L}{l^*}\eta)+\frac{4}{3}\eta\cosh(\frac{L}{l^*}\eta)}{\sinh(\alpha^*\eta)+\frac{2}{3}\eta\cosh(\alpha^*\eta)}\left[\sinh(\alpha^*\chi)+\frac{2}{3}\chi\cosh(\alpha^*\chi)\right]}{\left(1+\frac{4}{9}\chi^2\right)\sinh\left(\frac{L}{l^*}\chi\right)+\frac{4}{3}\chi\cosh\left(\frac{L}{l^*}\chi\right)}, \tag{11}$$

where $\eta = \sqrt{3l^*/l_a}$, $\alpha^* = z_0/l^*$, and $\chi = \sqrt{k_0^2\langle\Delta r^2(t)\rangle + \eta^2}$.

It is important to note that this formula is more complicated than Eq. (4) because the normalization term is quite different. However, when $l_a \to \infty$, the original expression for the ACF is recovered, that is, for the case of no absorption [Eq. (4)]. As pointed out previously, absorption effects can be taken into account using a proper variable change directly in Eq. (5) as described in [2,3] or using the approximation expression of the intensity correlation function proposed by Rojas-Ochoa *et al.* [46]. However, the procedure just explained formally retrieves the correct form of the ACF.

As a consequence, measuring the intensity ACF, $g_{(2)}(t)$, for the scattered light of microspheres in random motion embedded in a fluid, and by numerical inversion of Eq. (11), the MSD of the microspheres can be obtained when light absorption in the fluid of interest cannot be neglected. The Siegert relation, $g_{(2)}(t) = 1 + \beta|g_{(1)}(t)|^2$, has to be employed, where β is a correction factor that depends on the geometry, to get the MSD of the particles.

3. Materials and Methods

A. Materials

Polystyrene microspheres of 140 nm were purchased from Bangs Laboratories Inc. (Fishers, Indiana). The weight concentration of the microsphere vial solutions was obtained by gravimetric measurements after total solvent evaporation on solution aliquots. Milli-Q water (nanopure-UV, USA; 18.3 MΩ) was used for sample preparation. Rectangular glass cells ($L = 2500$ μm) were supplied by Starna Cells Inc. (USA). Specific amounts of a dilute India ink solution (1 wt. %) were added to the microsphere sample solutions as a light-absorbing agent.

B. Optical Parameters Recovery

Reflectance and transmittance measurements were performed on samples with embedded microspheres, where specific quantities of light-absorbing agent were added, using an integrating sphere (Oriel Newport, USA). The integrating sphere employs a photomultiplier tube (Hamamatsu Ltd., Japan) attached at the wall sphere, and laser light at a wavelength of $\lambda = 514.5$ nm (Coherent Innova 300, Coherent Inc., USA) was employed. Scattering and absorption coefficients (l^* and l_a) of the samples were recovered using the inverse adding doubling (IAD) method [47,48]. In the IAD method, a general numerical solution for the radiative transport equation is given through the following steps: (1) A guess for a set of optical parameters is given. (2) The reflection and transmission of the samples are evaluated using the adding doubling method developed by van de Hulst [49,50]. (3) Transmission and reflectance are compared with the experimental measurements. (4) If the match is not good enough, the set of optical parameters is modified using a minimization algorithm. This process is iteratively followed until a match with the experimental measurements at some specific level is made. IAD also takes into account several features experimentally difficult to assess, such as light lost out the edges and nonlinear effects in the integrating sphere measurements [48]. The results were compared with predictions coming from Mie's theory for the scattering coefficient, calculated from the estimated volume fraction taking into account the weighted amounts of water and polystyrene particles added to the solution [41,43]; the refractive index of particles = 1.59. In addition, a direct Monte Carlo simulation using a modified version of the Monte Carlo multilayer algorithm [51] was employed, allowing us to calculate the light lost by the edges of the sample as well as the amount of light absorbed by the sample. A second method for optical parameter recovery was used to estimate the scattering coefficient based on the light diffusion approximation without absorption [52]. However, their results completely fail with respect to the Mie's theory.

C. DWS

Our experimental setup is described elsewhere [53]; here just a brief description is given based on Fig. 1. Light from a laser (Coherent Innova 300, Coherent Inc., USA) is filtered and expanded to ensure the plane wave approximation and subsequently sent at normal incidence on the sample kept in a temperature-controlled bath. All measurements were made at a temperature of 25°C. Scattered light is collected by photomultiplier tubes (Thorn EMI, England) through an optical fiber (OZoptics Inc., USA). Preamplifiers and a ALV/5000E multi-tau correlator (ALV GmbH, Germany) convert signals into transistor–transistor logic (TTL) pulses and compute the intensity correlation functions in cross correlation, respectively. Typical acquiring times are around 1800 s.

4. Results and Discussion

Figure 2 shows an example for total reflectance, transmittance, lateral escape, and absorption as a function of l_a for five samples where small amounts of India ink solution were added to increase their absorption. The samples were prepared for tentatively different l_i^* ranging approximately from 100 to 250 μm. Actual recovered values will be presented below. For all cases, $L/l^* \geq 10$ to ensure that the diffusion approximation for light propagation within

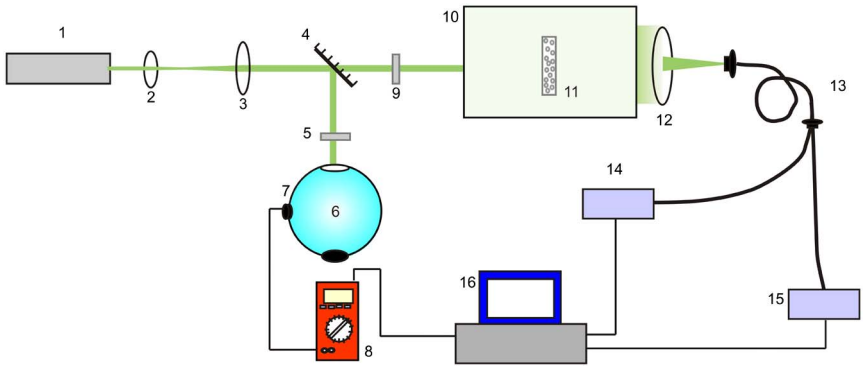

Fig. 1. Experimental setup: 1, Ar^+ laser; 2 and 3, beam expander; 4, movable mirror; 5, attenuator; 6, integrating sphere; 7, detector; 8, voltmeter; 9, polarizer; 10, thermal bath; 11, sample; 12, lens; 13, optical fiber; 14 and 15, photomultiplier tube; 16, computer with correlator.

the sample always holds [43]. l_a was recovered from reflectance and transmittance measurements using the integrating sphere [47,48]. Absorption-free samples have an absorption length of around 30,000 mm; the uncertainty of this value is large using our procedure; however, this value roughly corresponds to water absorption [54]. Absorption and lateral escape were estimated using the Monte Carlo algorithm mentioned above. In a scattering medium without absorption, a decrease in the transmittance is related to a decrease in the transport mean free path, but reflectance increases proportionally in such a way that $R + T$ remains mostly unchanged. In a scattering and absorbing turbid medium, by increasing absorption thorough increasing the concentration of the absorbing agent, the reflectance and transmittance decrease, no matter the approximate value of l^*, as observed in Fig. 2. As expected, absorption increases as the added India ink increases, up to a value of 60% for sample E and $l_a = 4.1$ mm. Lateral escape decreases with the increase of the absorption agent in a similar way to transmittance, and apparently it is not sensitive to the l^* value.

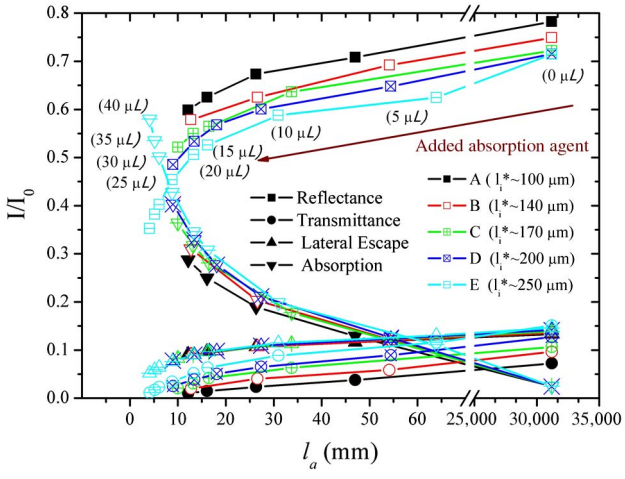

Fig. 2. Reflectance, transmittance, lateral escape, and absorption as functions of l_a, where ~5 μl of a dilute 1% solution of India ink was added successively to all the samples starting from right to left. Ink was not added to the first point of each curve.

Figure 3 shows recovered values of l^* as a function of recovered values of l_a for the samples presented in Fig. 2. Filled symbols correspond to the optical parameters recovered with IAD [48], and dashed lines correspond to Mie predictions for l^* obtained from the microsphere volume fraction of the samples [41,43]. In samples with a higher absorption coefficient, the corresponding added volume of ink solution was taken into account to carry out the Mie calculation. As can be observed, recovered l^* values using the IAD method agree with Mie's theory within the experimental error, except for the case of l^* for $l_a = 16.5$ mm in the sample labeled as C; this value seems abnormally above the Mie prediction. This might correspond to a laser misalignment during the total transmittance measurement, because it is the only measurement far away from Mie's theory.

Figure 4(a) shows an example of the normalized ACFs for the scattered light coming from solutions of microspheres that contain different absorbing agent concentrations. The curves span from a solution with no added absorbing agent ($l_a \approx 30{,}000$ mm) up to a sample with a $l_a = 4.1$ mm and with a transport mean free path of $l^* \approx 250$ μm. As expected, the time delay in the correlation functions shifts to longer

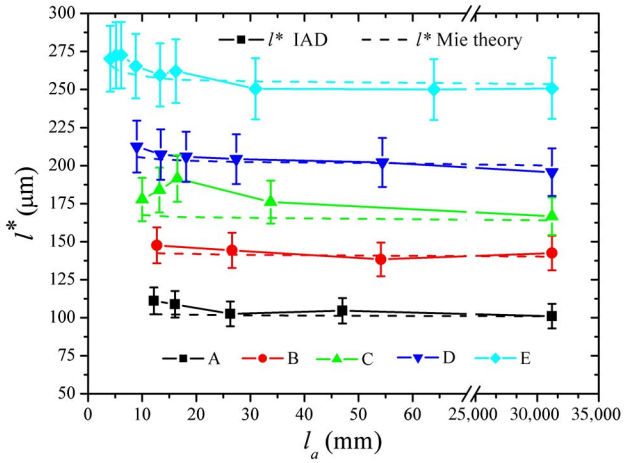

Fig. 3. l^* recovered using IAD with reflectance and transmittance measurements, and predictions of Mie's theory.

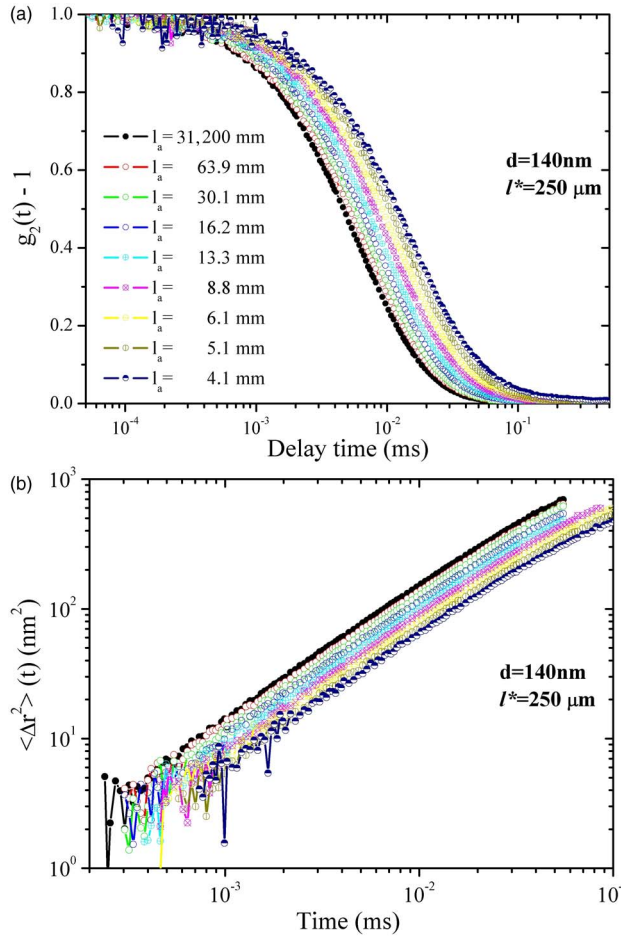

Fig. 4. Intensity ACFs and MSDs. (a) Normalized intensity autocorrelation as the absorbing agent concentration increases for $l^* = 250$ μm. The increase of absorbing agent displaces the correlation function to the right. (b) MSDs obtained from the intensity correlations functions presented in (a) [using Eq. (4)]. Labels are the same as in (a). The increase of absorbing agent displaces the MSD curves to the right.

times as absorption increases. We found a similar trend in all measured samples, no matter the transport mean free path (data not shown). Figure 4(b) presents the wrong MSD, which would be obtained by numerical inversion of Eq. (4) using the ACFs shown in Fig. 4(a). If the data are not corrected by the absorption contribution, the shift in ACF delay time would be interpreted in DWS as a change in the colloidal dynamics of the scattering particles.

To make more clear how the correlation function is modified due to absorption, from the correlation functions of Fig. 4, we measured the time lag difference from the absorbing samples at a high of $g_{(2)}(t) = 0.2$, and a chart was made for this time lag, t_{lag} versus l_a; see Fig. 5. For particles diffusing in Brownian motion, the time delay shift is inversely proportional to l_a [see Eq. (5)]; this is the trend observed in Fig. 5. From the time delay shift, some authors have estimated the transport mean free path and/or the absorption length by computing the distribution of paths of length s, that is, $P(s)$ [35,36]; this

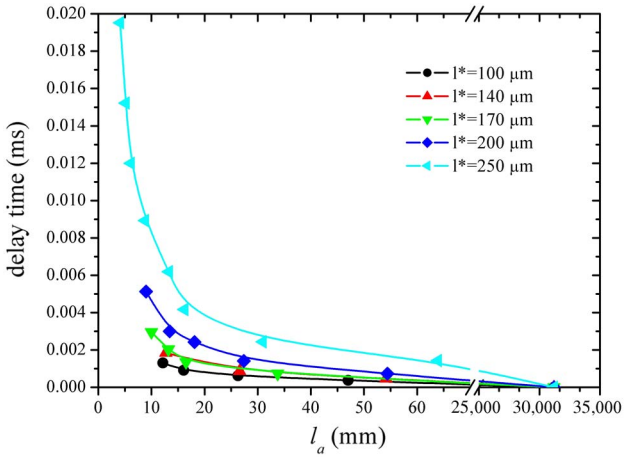

Fig. 5. Time delay of the ACF at $g_{(2)}(t) = 0.2$ with respect to the case of no absorption for different values of l_a.

technique is called diffusing wave absorption spectroscopy. Our data can be analyzed in a similar way; however, the applicability of this technique is restricted to particles diffusing in Brownian motion, where the absorption effects in DWS are just seen as

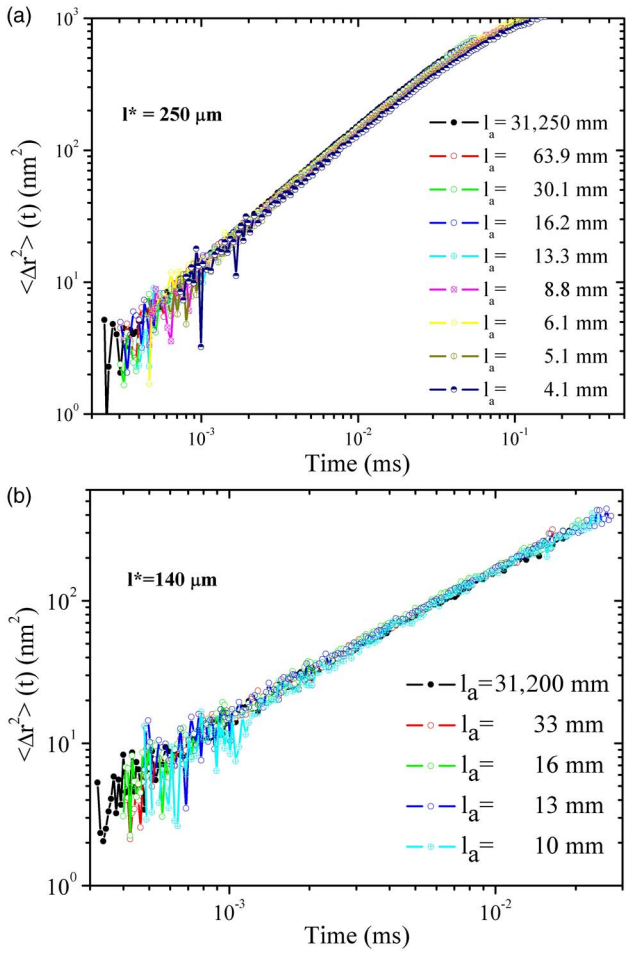

Fig. 6. Corrected MSDs of particles in Brownian motion embedded in an absorbing medium characterized by $l^* = 140$ and 250 μm. The corrected MSDs were obtained from the correlation functions given in Fig. 4 and employing Eq. (11).

a time delay shift inversely proportional to the absorption length. However, Eq. (11) is general and can be used for extracting the MSD from any turbid absorbing medium.

By including in DWS experiments absorption effects, as in Eq. (11), the true MSDs can be calculated from the experimental intensity ACFs presented in Fig. 4. The corrected MSD versus t curves for $l^*\approx 140$ μm are shown in Fig. 6(a), and in Fig. 6(b) for $l^*\approx 250$ μm. As can be seen, this version of DWS that includes absorption gives the same MSD for particles in Brownian motion no matter the absorption length; this is valid for $l^*\approx 100$, 170, and 200 μm (data not shown). However for the sample with $l^*\approx 250$ μm, some differences in the MSD are observed in the samples with a higher concentration of absorbing agent. In particular, for $l_a = 6.1$ mm, the MSD not only shifts to longer times, but it presents an inflexion point. The diffusion approximation for light propagation is adequate for a scattering turbid medium, with $l_a \gg l^*$. This occurs for the samples in Fig. 6(b), where $l_a/l^* > 66$ and $L/l^* > 10$. However, for the samples in Fig. 6(a), we found that when $l_a/l^* \leq 24$ and $L/l^* \sim 10$, that is, close to the limit of validity of the diffusion approximation, our correction fails. In this case, we suspect that the diffusion approximation is no longer valid for modeling light in this turbid medium. We set the turning point of our experiments at approximately $l_a/l^* \geq 10$ and $L/l^* > 10$.

About the discussion related to the diffusion equation involving a diffusion coefficient independent of the absorption, D_1, or dependent on the absorption $[D_2 = c(l^* + l_a)/3]$, mentioned above, it is important to mention that we made a comparison for $g_{(2)}(t)$ calculated using both expressions of the diffusion coefficient. The difference is negligible since $l_a \gg l^*$.

5. Conclusion

The colloidal dynamics in complex fluids with absorption using DWS seem to be slower, thus producing incorrect microrheology results if corrections are not considered. By increasing absorption, the ACF of the scattered light shifts to longer lag times because of the attenuation of the long paths of photons. As expected, the time lag shift is inversely proportional to the absorption length. Absorption can be included straightforwardly using a proper diffusion equation for the photon propagation. The path distribution function is attenuated exponentially with respect to the case of no absorption. Here, we proposed an expression for the time-averaged light intensity ACF that correctly describes the time fluctuations, where the diffusion approximation accurately describes the light propagation within the sample. The time fluctuations of the scattered light were related to the MSD of the embedded particles. The correct colloidal dynamics in the turbid medium were evaluated and experimentally assessed. This result extends the applicability of DWS for systems where absorption cannot be neglected, and it opens the possibility of doing microrheology with this optical method in systems where absorption cannot be avoided.

We thank C. Garza for her technical support. Funding from SEP-CONACYT (177679) and DGAPA-UNAM (IN 110414) are gratefully acknowledged.

References

1. G. Maret and P. E. Wolf, "Multiple light scattering from disordered media: the effect of Brownian motion of scatterers," Z. Phys. B **65**, 409–413 (1987).
2. D. J. Pine, D. A. Weitz, P. M. Chaikin, and E. Herbolzheimer, "Diffusing-wave spectroscopy: dynamic light scattering in the multiple scattering limit," Phys. Rev. Lett. **60**, 1134–1137 (1988).
3. D. A. Weitz and D. J. Pine, "Diffusing-wave spectroscopy," in *Dynamic Light Scattering*, W. Brown, ed. (Oxford University, 1993), p. 652.
4. D. J. Pine, D. A. Weitz, J. X. Zhu, and E. Herbolzheimer, "Diffusing-wave spectroscopy: dynamic light scattering in the multiple scattering limit," J. Phys. (Paris) **51**, 2101–2127 (1990).
5. D. D. Kaplan, M. H. Kao, A. Yodh, and D. Pine, "Geometric constraints for the design of diffusing-wave spectroscopy experiments," Appl. Opt. **32**, 3828–3836 (1993).
6. J. L. Harden and V. Viasnoff, "Recent advances in DWS-based micro-rheology," Curr. Opin. Colloid Interface Sci. **6**, 438–445 (2001).
7. J. Li, G. Dietsche, D. Iftime, S. E. Skipetrov, G. Maret, T. Rockstroh, and T. Gisler, "Noninvasive detection of functional brain activity with near-infrared diffusing-wave spectroscopy," J. Biomed. Opt. **10**, 044002 (2005).
8. F. Jaillon, S. E. Skipetrov, J. Li, G. Dietsche, G. Maret, and T. Gisler, "Diffusing-wave spectroscopy from head-like tissue phantoms: influence of a non-scattering layer," Opt. Express **14**, 10181–10194 (2006).
9. M. B. M. Ninck, G. Hering, L. Spinelli, D. C. A. Torricelli, and T. Gisler, "Noninvasive observation of skeletal muscle contraction using near-infrared time-resolved reflectance and diffusing-wave spectroscopy," J. Biomed. Opt. **15**, 057007 (2010).
10. M. Ninck, M. Untenberger, and T. Gisler, "Diffusing-wave spectroscopy with dynamic contrast variation: disentangling the effects of blood flow and extravascular tissue shearing on signals from deep tissue," Biomed. Opt. Express **1**, 1502–1513 (2010).
11. T. Durduran, R. Choe, G. Yu, C. Zhou, J. C. Tchou, B. J. Czerniecki, and A. G. Yodh, "Diffuse optical measurement of blood flow in breast tumors," Opt. Lett. **30**, 2915–2917 (2005).
12. G. Yu, T. Durduran, C. Zhou, T. C. Zhu, J. C. Finlay, T. M. Busch, S. B. Malkowicz, S. M. Hahn, and A. G. Yodh, "Real-time in situ monitoring of human prostate photodynamic therapy with diffuse light," Photochem. Photobiol. **82**, 1279–1284 (2006).
13. U. Sunar, S. Makonnen, C. Zhou, T. Durduran, G. Yu, H.-W. Wang, W. M. F. Lee, and A. G. Yodh, "Hemodynamic responses to antivascular therapy and ionizing radiation assessed by diffuse optical spectroscopies," Opt. Express **15**, 15507–15516 (2007).
14. Y. Shang, Y. Zhao, R. Cheng, L. Dong, D. Irwin, and G. Yu, "Portable optical tissue flow oximeter based on diffuse correlation spectroscopy," Opt. Lett. **34**, 3556–3558 (2009).
15. Y. Shang, T. B. Symons, T. Durduran, A. G. Yodh, and G. Yu, "Effects of muscle fiber motion on diffuse correlation spectroscopy blood flow measurement during exercise," Biomed. Opt. Express **1**, 500–511 (2010).
16. G. Dietsche, M. Ninck, C. Ortolf, J. Li, F. Jaillon, and T. Gisler, "Fiber-based multispeckle detection for time-resolved diffusing-wave spectroscopy: characterization and application for blood flow detection in deep tissue," Appl. Opt. **46**, 8506–8514 (2007).

17. F. Jaillon, J. Li, G. Dietsche, T. Elbert, and T. Gisler, "Activity of the human visual cortex measured non-invasively by diffusing-wave spectroscopy," Opt. Express **15**, 6643–6650 (2007).
18. G. Maret, "Diffusing-wave spectroscopy," Curr. Opin. Colloid Interface Sci. **2**, 251–257 (1997).
19. T. Gisler and D. A. Weitz, "Tracer microrheology in complex fluids," Curr. Opin. Colloid Interface Sci. **3**, 586–592 (1998).
20. F. C. MacKintosh and C. F. Schmidt, "Microrheology," Curr. Opin. Colloid Interface Sci. **4**, 300–307 (1999).
21. A. Mukhhopadhyay and S. Granick, "Micro- and nanorheology," Curr. Opin. Colloid Interface Sci. **6**, 423–429 (2001).
22. F. Scheffold, S. Romer, F. Cardinaux, H. Bissig, A. Stradner, L. F. Rojas-Ochoa, V. Trappe, C. Urban, S. E. Skipetrov, L. Cipelletti, and P. Schurtenbeger, "New trends in optical microrheology of complex fluids and gels," Prog. Colloid Polym. Sci. **123**, 141–146 (2004).
23. N. Willenbacher and C. Oelschlaeger, "Dynamics and structure of complex fluids from high frequency mechanical and optical rheometry," Curr. Opin. Colloid Interface Sci. **12**, 43–49 (2007).
24. T. D. Squires and T. G. Mason, "Fluid mechanics of microrheology," Annu. Rev. Fluid Mech. **42**, 413–438 (2010).
25. D. Lopez-Diaz and R. Castillo, "Microrheology of solutions embedded with thread-like supramolecular structures," Soft Matter **7**, 5926–5937 (2011).
26. A. P. Y. Wong and P. Wiltzius, "Dynamic light scattering with a CCD camera," Rev. Sci. Instrum. **64**, 2547–2549 (1993).
27. L. Cipelleti and D. A. Weitz, "Ultralow-angle dynamic light scattering with a charge coupled device camera based multispeckle, multitau correlator," Rev. Sci. Instrum. **70**, 3214–3221 (1999).
28. S. Kirsch, V. Frenz, W. Schartl, E. Bartsch, and H. Sillescu, "Multispeckle autocorrelation spectroscopy and its application to the investigation of ultraslow dynamical processes," J. Chem. Phys. **104**, 1758–1761 (1996).
29. M. Oda, Y. Yamashita, G. Nishimura, and M. Tamura, "Quantitation of absolute concentration change in scattering media by the time-resolved microscopic Beer–Lambert law," Adv. Exp. Med. Biol. **345**, 861–870 (1992).
30. P. E. Wolf, G. Maret, E. Akkermans, and R. Maynard, "Optical coherent backscattering by random media: an experimental study," J. Phys. **49**, 63–75 (1988).
31. L. T. Perelman, J. Wu, I. Itzkan, and M. S. Feld, "Photon migration in turbid media using path integrals," Phys. Rev. Lett. **72**, 1341–1344 (1994).
32. S. L. Jacques, "Time-resolved reflectance spectroscopy in turbid tissues," IEEE Trans. Biomed. Eng. **36**, 1155–1161 (1989).
33. S. L. Jacques, "Time resolved propagation of ultrashort laser pulses with turbid tissues," Appl. Opt. **28**, 2223–2229 (1989).
34. Y. Hasegawa, Y. Yamada, M. Tamura, and Y. Nomura, "Monte Carlo simulation of light transmission through living tissues," Appl. Opt. **30**, 4515–4520 (1991).
35. G. Nishimura, K. Katayama, M. Kinjo, and M. Tamura, "Diffusing-wave absorption spectroscopy in homogeneous turbid media," Opt. Commun. **128**, 99–107 (1996).
36. K. Katayama, G. Nishimura, M. Kinjo, and M. Tamura, "Absorbance measurements in turbid media by the photon correlation method," Appl. Opt. **34**, 7419–7427 (1995).
37. K. Furutsu and Y. Yamada, "Diffusion approximation for a dissipative random medium and the applications," Phys. Rev. E **50**, 3634–3640 (1994).
38. T. Durduran, A. G. Yodh, B. Chance, and D. A. Boas, "Does the photon-diffusion coefficient depend of absorption?" J. Opt. Soc. Am. A **14**, 3358–3365 (1997).
39. M. Bassani, F. Martelli, G. Zaccanti, and D. Contini, "Independence of the diffusion coefficient from absorption: experimental and numerical evidence," Opt. Lett. **22**, 853–855 (1997).
40. T. Nakai, G. Nishimura, K. Yamamoto, and M. Tamura, "Expression of optical diffusion coefficient in high-absorption turbid media," Phys. Med. Biol. **42**, 2541–2549 (1997).
41. A. Ishimaru, *Wave Propagation and Scattering in Random Media* (Academic, 1978).
42. R. Aronson and N. Corngold, "Photon diffusion coefficient in an absorbing medium," J. Opt. Soc. Am. A **16**, 1066–1071 (1999).
43. L. V. Wang and H. Wu, *Biomedical Optics: Principles and Imaging* (Wiley, 2007).
44. S. Chandrasekhar, "Stochastic problems in physics and astronomy," Rev. Mod. Phys. **15**, 1–89 (1943).
45. M. S. Patterson, B. Chance, and B. C. Wilson, "Time resolved reflectance and transmittance for the non-invasive measurement of tissue optical properties," Appl. Opt. **28**, 2331–2336 (1989).
46. L. F. Rojas-Ochoa, S. Romer, F. Scheffold, and P. Schurtenberger, "Diffusing wave spectroscopy and small-angle neutron scattering from concentrated colloidal suspensions," Phys. Rev. E **65**, 051403 (2002).
47. S. A. Prahl, M. J. C. van Gemert, and A. J. Welch, "Determining the optical properties of turbid media by using the adding–doubling method," Appl. Opt. **32**, 559–568 (1993).
48. S. A. Prahl, Inverse Adding Doubling, http://omlc.ogi.edu/software/iad/index.html.
49. H. C. van de Hulst, *Multiple Light Scattering* (Academic, 1980), Vol. **1**.
50. H. C. van de Hulst, *Multiple Light Scattering* (Academic, 1980), Vol. **2**.
51. B. M. Cruzado, S. V. y Montiel, and J. A. D. Atencio, "Genetic algorithms and MCML program for recovery of optical properties of homogeneous turbid media," Biomed. Opt. Express **4**, 433–446 (2013).
52. J. Galvan-Miyoshi and R. Castillo, "Absolute values of transport mean free path of light in non-absorbing media using transmission and reflectance measurements," Rev. Mex. Fis. **54**, 257–264 (2008).
53. J. Galvan-Miyoshi, J. Delgado, and R. Castillo, "Diffusing wave spectroscopy in Maxwellian fluids," Eur. Phys. J. E **26**, 369–377 (2008).
54. G. M. Hale and M. R. Querry, "Optical constants of water in the 200 nm to 200 m wavelength region," Appl. Opt. **12**, 555–563 (1973).